ACS Sustainable Chemistry & Engineering

Research Article

pubs.acs.org/journal/ascecg

Periodic Mesoporous Silica-Supported Scandium Triflate as a Robust and Reusable Lewis Acid Catalyst for Carbon−Carbon Coupling Reactions in Water

Mingzhen Chen, Chao Liang, Fang Zhang,* and Hexing Li*

The Education Ministry Key Lab of Resource Chemistry and Shanghai Key Laboratory of Rare Earth Functional Materials, Shanghai Normal University, Shanghai 200234, P. R. China

Supporting Information

ABSTRACT: Phenyl-bridged periodic mesoporous organosilica modified with sodium benzenesulfonate groups ($NaSO_3Ph$-PMO) was frabicated by template-assembled co-condensation and subsequent ion-exchange processes. This functionalized support efficiently anchored scandium triflate to generate a mesoporous Lewis acid catalyst ($Sc(OTf)_2$-SO_3Ph-PMO). It exhibited superior catalytic reactivity compared to those of the homogeneous catalyst scandium triflate and $Sc(OTf)_2$-SO_3Ph-SBA-15, without the phenyl groups inside the mesoporous wall of the water medium Barbier−Grignard and Mukaiyama−Aldol reactions. The physico−chemical characterizations demonstrated that its excellent catalytic performance was due to its ordered mesoporous channel and hydrophobicity microenvironment, which could stabilize and concentrate the substances as well as decrease intrinsic mass transfer resistance. Furthermore, the $Sc(OTf)_2$-SO_3Ph-PMO catalyst retained high catalytic reactivity even after 10 reuses, confirming its excellent catalytic stability.

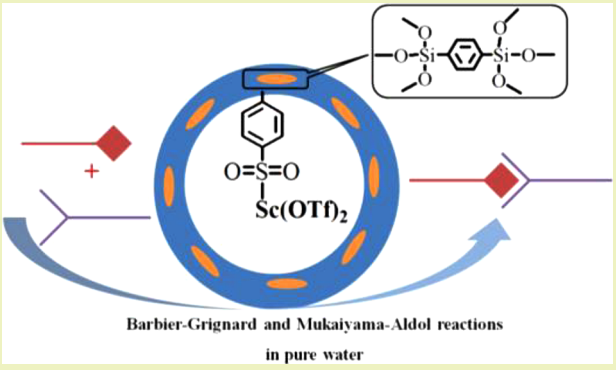

KEYWORDS: *Periodic mesoporous silica, Scandium triflate, Lewis acid, Water medium organic synthesis*

INTRODUCTION

Increasing fossil reserve consumption and environmental concerns require scientists to develop new green and sustainable science and technology for chemical transformations.[1] It has become increasingly important to develop economical and sustainable synthetic methodologies that help to conserve our limited natural resources.[2] One effective way to surmount these challenges is to discover and use highly active and stable heterogeneous catalysts because they generally allow for the decreased use of toxic reagents, reduced discharge of waste, and easy operation of the reaction system.[3] Among heterogeneous catalysts, solid acids are one of the most important industrial catalysts for a variety of key chemical processes.[4] In addition, the use of water as a green solvent in solid acid-catalyzed organic synthesis has attracted much interest recently.[5−11] However, decreased activity was often observed when efficient homogeneous acid catalysts were immobilized because of the poor solubility of many organic compounds in water.[12] In particular, the traditional Lewis acids like $AlCl_3$ and BF_3 are decomposed into their metal hydroxide in water and accordingly lose their catalytic reactivities.[13−15] While some solid Lewis acids were known to work well in aqueous media, there are still many hurdles that need to be overcome such as unsatisfactory catalytic efficiency and limited reaction types and substrates.[16−29] Therefore, the design and synthesis of highly active and stable solid Lewis acids for aqueous organic reactions are urgently needed.

Periodic mesoporous organosilica (PMO) represents an exciting new class of hybrid organic−inorganic materials in different fields such as separation[30] and catalysis.[31,32] Among PMO materials, those incorporating benzene bridges have attracted great interest owing to their crystal-like pore wall structure and hydrophobic phenyl layer inside the pore wall.[33] Recently, several research groups have shown that sulfonated periodic mesoporous benzenesilica material (Ph-PMO-SO_3H) was much more stable and more active than conventionally used solid acid catalysts such as zeolites, cation exchange resins, and sulfonated mesoporous silica for various organic reactions in water.[34−36] Their increased reactivity and recyclability were attributed to the large amount of propyl-SO_3H groups anchored in the mesopore channels together with the hydrophobic benzene groups embedded in the mesoporous wall. This unique physical structure and chemical composition favor the transportation of the reactants and protect the acidic sites against water salvation. However, water-compatible Lewis acids supported on benzene-bridged PMO materials have not

Received: September 30, 2013
Revised: November 25, 2013
Published: December 2, 2013

Scheme 1. Illustration of $Sc(OTf)_2$-SO_3Ph-PMO Catalyst Preparation

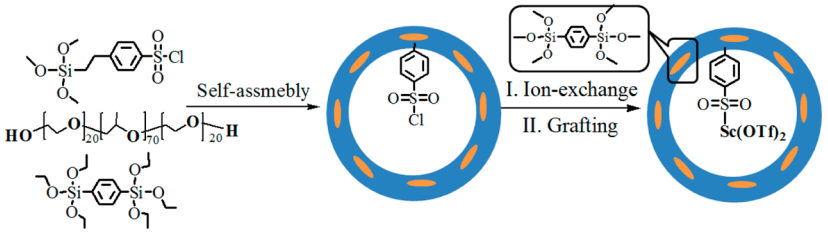

yet been investigated.[37−39] Herein, we reported our efforts to immobilize scandium triflate in the benzene-bridged sodium benzenesulfonate PMO support that was synthesized by surfactant-directed assembly between 2-(4-chlorosulphonylphenyl)ethyl trimethoxylsilane and 1,4-bis-(triethoxysilyl)benzene. This modified Lewis acid exhibited excellent catalytic reactivity and selectivity in water medium Barbier−Grignard and Mukaiyama−Aldol reactions. Further, it could be easily reused and recycled at least 10 times.

EXPERIMENTAL SECTION

Material Preparation. *Fabrication of Sodium Benzenesulfonate-Functionalized Benzene-Bridged PMO ($NaSO_3Ph$-PMO).* $NaSO_3Ph$-PMO support was prepared through a two-step process (Scheme 1). First, $ClSO_3Ph$-functionalized PMO was synthesized through one-step template-directed assembly approach between 2-(4-chlorosulphonylphenyl)ethyl trimethoxylsilane (CSPTS) and 1,4-bis(triethoxysilyl)benzene (BTEB). In a typical synthesis, 3.56 mL BTEB was added into an aqueous solution composed of 2.0 g of P123, 6.0 g of KCl, and 80 mL of 0.2 M HCl at 40 °C. After stirring for 1.0 h, 0.64 mL of CSPTS was introduced into the reaction mixture and allowed to stir for 1.0 d. Subsequently, the mixture was added into a 200 mL Teflon bottle and left at 100 °C for 1.0 d. The solid sample was separated and washed with water and ethanol. The template P123 was removed by ethanol extraction at 80 °C, and the solid product was achieved by vacuum drying. Then, 1.0 g of dried powder was redispersed in 50 mL of water, and the temperature was increased to 60 °C. After stirring for 6.0 h, a certain amount of 0.1 M $NaHCO_3$ was added into the above mixture until the pH value of the solution reached 7.0. Accordingly, the solid product was centrifuged, washed with water, dried in vacuum, and denoted as $NaSO_3Ph$-PMO.

Frabication of PMO-Supported Lewis Acid Catalyst ($Sc(OTf)_2$-SO_3Ph-PMO). A total of 1.0 g of $NaSO_3Ph$-PMO was added into 50 mL of ethanol containing 0.50 g of scandium triflate ($Sc(OTf)_3$, OTf = $-SO_3CF_3$). The mixture was allowed to react at 60 °C for 1.0 d. Then, the catalyst was separated and treated with ethanol washing to remove the uncoordinated scandium triflate.

Characterization. Inductively coupled plasma optical emission spectrometer (Varian VISTA-MPX) was used to calculate the scandium content. Elemental analysis by using an Element Vario EL III analyzer determined the sulfur content. X-ray photoelectron spectroscopy was acquired on a Perkin-Elmer PHI 5000C ESCA to obtain the electronic states of various elements. The binding energy values were calibrated by using C_{1S} = 284.6 eV as a reference. X-ray powder diffraction (XRD) was obtained on a Rigaku D/maxr B diffractometer using Cu Kα radiation. N_2 sorption isotherms were used to obtain the pore structure information with a Quantachrome NOVA 4000e analyzer. Transmission electron microscopy was operated on a JEM2011 microscope at 200 kV.

Activity Test. *Barbier−Grignard Reaction.* In each run of the Barbier−Grignard reactions, 0.025 mmol Sc(III) catalyst, 53 mg of benzaldehyde (0.5 mmol), 331 mg of allyl-tri-n-butaltin (1.0 mmol), and 5.0 mL of distilled water were added in a flask and then increased in temperature to 80 °C. After stirring for 24 h, the mixture was extracted by ethyl acetate and then analyzed on a gas chromatograph (GC, Agilent 1790). The conversion was determined by the remaining benzaldehyde amount. The selectivity was determined by the ratio between the 1-phenyl-3-buten-1-ol amount determined by GC and the theoretical amount of 1-phenyl-3-buten-1-ol.

Mukaiyama−Aldol Reaction. In each run of the Mukaiyama−Aldol reactions, 0.050 mmol Sc(III) catalyst, 53 mg of benzaldehyde (0.50 mmol), 190 mg of trimethyl(1-phenylprop-1-enyloxy)silane (1.0 mmol), and 3.0 mL of distilled water were introduced in a flask, and the temperature was kept at 10 °C. After mild stirring for 27 h, the mixture was extracted with toluene and then analyzed on a high performance liquid chromatography analyzer (HPLC, Agilent 6410 series Triple Quad) equipped with an Agilent C_{18} column. The conversion was determined by the remaining benzaldehyde amount.

Determination of Catalyst Leaching and Durability. To determine the catalyst recyclability of the Sc-based mesoporous catalysts, we separated the catalyst by centrifugation after each run of reaction was finished. The solid catalysts were dried in vacuum and then charged with the reactants and solvent for the following recycled experiments under the same reaction conditions. In all the catalytic tests, we checked the reproducibility by repeating the activity data at least three times, and the difference in the catalytic result was found to be within ±5%.

Adsorption Test. To test the adsorption behaviors of different Sc-based mesoporous catalysts, we soaked mesoporous Sc catalyst (50 mg) in water (50 mL) and then oscillated this solution at 25 °C for 12 h. Subsequently, we added 50 mg/L of benzaldehyde aqueous solution (50 mL) into the mixture. We calculated the concentration of the benzaldehyde remaining in the mixture at a certain time interval on a HPLC analyzer (Agilent 6410 series Triple Quad) equipped with an Agilent C_{18} column. The adsorption capacity of various Sc-based mesoporous catalysts was calculated after benzaldehyde reached its saturation adsorption.

RESULTS AND DISCUSSION

To illustrate the successful synthesis of the PMO-supported rare earth Lewis acid catalyst, we characterized its chemical composition using Fourier-transform infrared spectroscopy (FT-IR) and X-ray photoelectron spectroscopy technology (XPS). The FTIR spectrum of the $Sc(OTf)_2$-SO_3Ph-PMO sample (Figure 1) revealed that it showed three additional absorption peaks compared to the pristine phenyl-bridged PMO support. One new peak around 579 cm^{-1} was attributed to the asymmetric bending absorption of CF_3 groups, while the peak at 1180 cm^{-1} was assigned to the asymmetric C−F stretching absorption of the CF_3 group. In addition, the sulfate stretching vibration absorption at 1255 cm^{-1} could also be found in the $Sc(OTf)_2$-SO_3Ph-PMO sample.[40] This result demonstrated the successful incorporation of the $Sc(OTf)_3$ complex in the PMO support. Furthermore, XPS spectra (Figure 2a) showed that the binding energy (BE) of the Sc element in the $Sc(OTf)_2$-SO_3Ph-PMO sample was 403.9 and 408.7 eV in $2P_{3/2}$ and $2P_{1/2}$ levels, respectively. This data confirmed that all the Sc species were of the trivalence oxidation state.[41] However, the Sc species in scandium triflate displayed that the binding energy was 404.4 and 409.2 eV in $2P_{3/2}$ and $2P_{1/2}$ levels, respectively. This difference could be explained based on the stronger electron-donating property of

dx.doi.org/10.1021/sc400391r | ACS Sustainable Chem. Eng. 2014, 2, 486−492

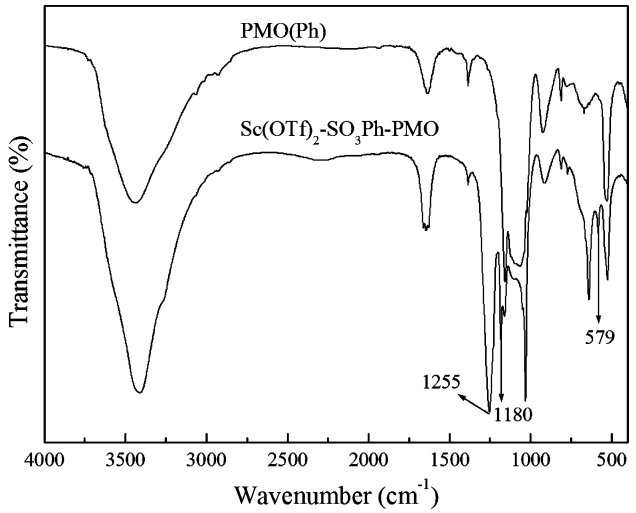

Figure 1. FTIR spectra of the pristine PMO(Ph) sample and $Sc(OTf)_2$-SO_3Ph-PMO catalyst.

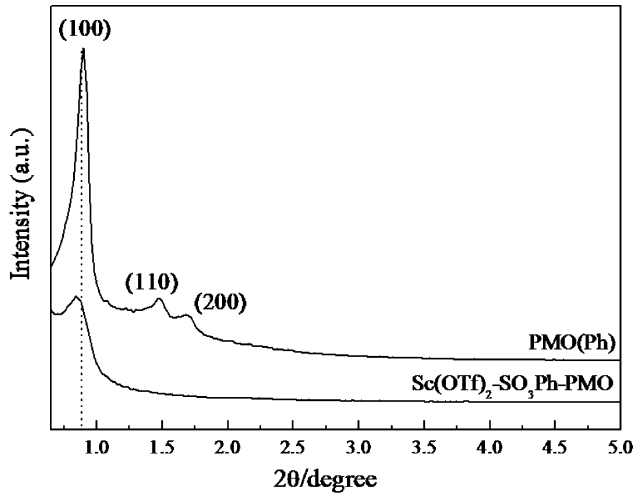

Figure 3. XRD spectra of PMO(Ph) and $Sc(OTf)_2$-SO_3Ph-PMO samples.

the sulfur element in benzenesulfonate groups compared to that in triflate ligands. A similar phenomena could be found in the XPS analysis of the sulfur element. The results showed that the BE of the S species in the $Sc(OTf)_2$-SO_3Ph-PMO sample shifted around 0.4 eV compared to that in scandium triflate.[42] On the basis of the above results, we suggested that scandium triflate was immobilized onto the functionalized PMO support by replacing one triflate ligand in $Sc(OTf)_3$ with the benzenesulfonate group incorporated in the mesoporous channels (Scheme 1).

The small-angle XRD pattern of the PMO(Ph) sample (Figure 3) exhibited one strong peak and two weak peaks, which could be assigned to (100), (110), and (200) reflections, respectively.[43] However, the $Sc(OTf)_2$-SO_3Ph-PMO sample displayed only one peak corresponding to the (100) reflection, and also, this peak shifted to a lower angle in comparison with pristine benzene-bridged PMO. This result demonstrated that the ordered hexagonal mesoporous structure (*p6mm*) could be retained for the $Sc(OTf)_2$-SO_3Ph-PMO sample; meanwhile, the existence of the Sc(II) complex inside the mesoporous channel increased the thickness of the mesoporous wall.[44] The ordered mesopore of the $Sc(OTf)_2$-SO_3Ph-PMO sample could be further confirmed by the TEM image, which showed that it had a two-dimensional hexagonal-arranged pore structure and a one-dimensional pore channel. The mesopore size of the $Sc(OTf)_2$-SO_3Ph-PMO sample was uniform and about 4.0 nm (Figure 4). Accordingly, $Sc(OTf)_2$-SO_3Ph-PMO exhibited the

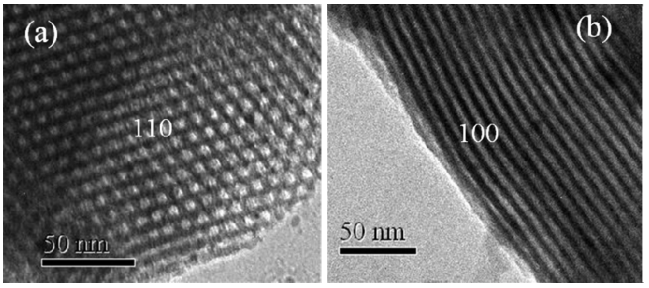

Figure 4. TEM images of $Sc(OTf)_2$-SO_3Ph-PMO sample.

type IV nitrogen sorption isotherm with a H_1 hysteresis loop, revealing its mesoporous structure (Figure 5). From Table 1, compared to the PMO(Ph) sample, the decrease in S_{BET}, D_P, and V_P of the $Sc(OTf)_2$-SO_3Ph-PMO sample showed that the Sc(III) complex in the grafted process was mainly located on internal surface of the mesoporous channels.[45]

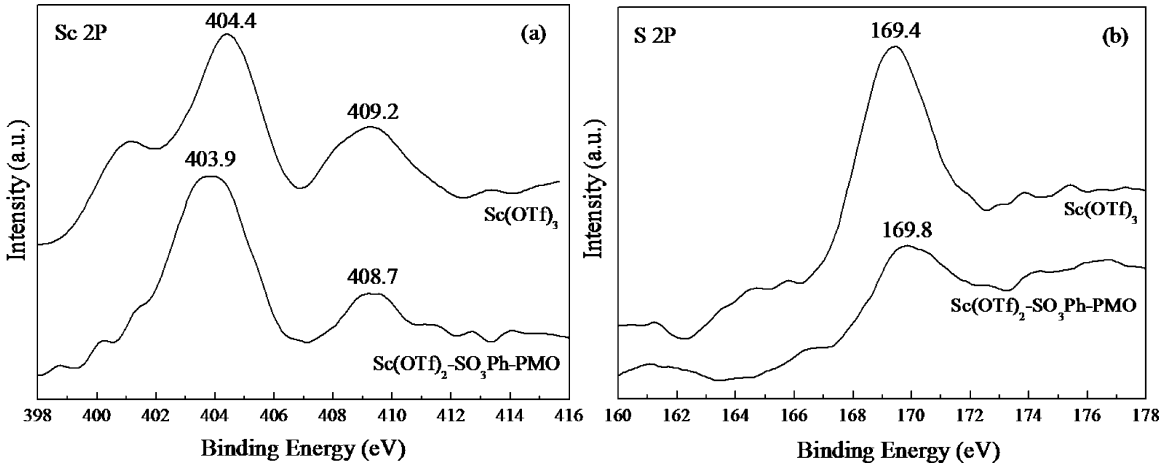

Figure 2. XPS spectra of $Sc(OTf)_3$ and $Sc(OTf)_2$-SO_3Ph-PMO samples.

dx.doi.org/10.1021/sc400391r | ACS Sustainable Chem. Eng. 2014, 2, 486−492

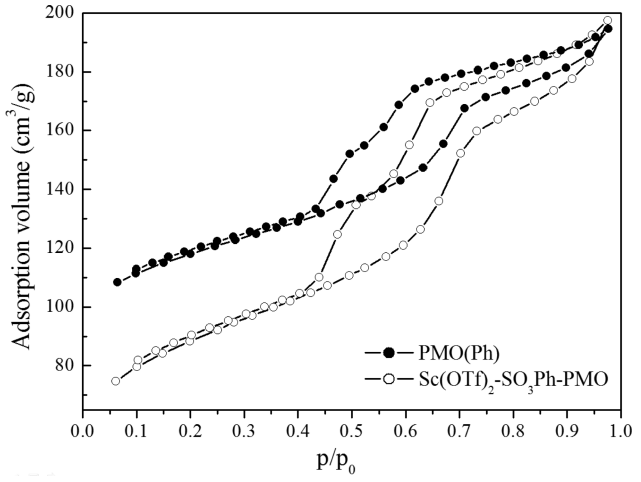

Figure 5. N_2 sorption isotherms of PMO(Ph) and $Sc(OTf)_2$-SO_3Ph-PMO samples.

Table 1. Structural Parameters of Phenyl-Bridged PMO and PMO-Supported Lewis Acid Catalysts

sample	S content (mmol/g)	Sc loading (mmol/g)	S_{BET} (m^2/g)	Vp (cm^3/g)	Dp (nm)
PMO(Ph)	–	–	615	0.78	4.1
$Sc(OTf)_2$-SO_3Ph-PMO	0.84	0.23	446	0.45	3.6
$Sc(OTf)_2$-SO_3Ph-PMO[a]	0.69	0.19	359	0.42	3.5
$Sc(OTf)_2$-SO_3Ph-SBA-15	0.81	0.22	555	1.1.	6.3

[a]After being reused 10 times.

We first used a water medium Barbier–Grignard reaction to evaluate the catalytic efficiencies of mesoporous Sc catalysts (Table 2). The control experiments indicated that the blank experiments could not give any products for the water medium Barbier–Grignard reaction. Moreover, for the $NaSO_3Ph$-PMO support, the slight increase in conversion for these two experiments could be attributed to its intrinsic weak acid property. However, the conversion was significant lower than that of the $Sc(OTf)_2$-SO_3Ph-PMO catalyst. These results clearly indicated that Sc^{3+} Lewis acid active sites were the active catalytic species. As shown in Table 2, the $Sc(OTf)_2$-SO_3Ph-PMO catalyst proceeded cleanly to the coupling product 1-phenyl-3-buten-1-ol with a 91% yield. In addition to the main product, 1-phenyl-3-buten-1-ol, the self-coupling byproduct of allyl-tri-n-butaltin, 1,5-hexadiene, was not identified in the reaction mixture. This suggested that the $Sc(OTf)_2$-SO_3Ph-PMO catalyst was highly selective. Interestingly, the homogeneous catalyst $Sc(OTf)_3$ displayed a slightly lower catalytic efficiency with an 85% yield in the same conditions. Next, we examined the scope of the $Sc(OTf)_2$-SO_3Ph-PMO-catalyzed Barbier–Grignard coupling on a series of substances. Similarly, 4-substituted benzaldehyde derivatives having either the electron-accepting group (NO_2–) or the electron-donating group (CH_3O–) also led to high yields of coupling products. Meanwhile, it exhibited a higher reactivity than that of the $Sc(OTf)_3$ catalyst in those reactions. This enhancement in catalytic activity of the $Sc(OTf)_2$-SO_3Ph-PMO catalyst was attributed to its high surface area and ordered mesoporous structure, which effectively stabilized and concentrated the substances, allowing the reaction to proceed smoothly in water. Moreover, the location of the phenyl groups in the framework created a favorable hydrophobic microenvironment, which was favorable for organic molecule diffusion.[46]

We also tested the catalytic efficiency of the reference catalyst $Sc(OTf)_2$-SO_3Ph-SBA-15 to further understand the catalytic behavior of the $Sc(OTf)_2$-SO_3Ph-PMO catalyst. As shown in Table 2, $Sc(OTf)_2$-SO_3Ph-SBA-15 displayed inferior catalytic efficiency with the same Sc loading in the water medium Barbier–Grignard reactions in comparison with the $Sc(OTf)_2$-SO_3Ph-PMO catalyst. Encouraged by these results, we also compared their catalytic activities in water medium Mukaiyama–Aldol reaction between benzaldehyde and trimethyl(1-phenylprop-1-enyloxy)silane. We first tested the blank experiment and the catalytic performances of the $NaSO_3Ph$-PMO support. The blank experiment indicated that no product could be detected; meanwhile, the $NaSO_3Ph$-PMO sample displayed very low yield (5.4%). As shown in Figure 6, the reaction files showed that the $Sc(OTf)_2$-SO_3Ph-PMO catalyst exhibited much higher yield (90%) than that of $Sc(OTf)_2$-SO_3Ph-SBA-15 with a 65% yield. To gain precise insight into the superior

Table 2. Water Medium Barbier–Grignard Reaction with Various Catalysts[a]

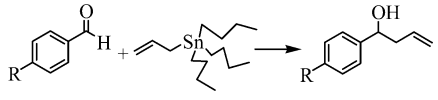

catalyst	R	conversion (%)	selectivity (%)	yield (%)
blank	H	0	0	0
$NaSO_3Ph$-PMO[b]	H	8.7	~100	8.7
$Sc(OTf)_3$	H	85	~100	85
$Sc(OTf)_2$-SO_3Ph-PMO	H	91	~100	91
$Sc(OTf)_2$-SO_3Ph-SBA-15	H	81	~100	81
$Sc(OTf)_3$	NO_2–	95	~100	95
$Sc(OTf)_2$-SO_3Ph-PMO	NO_2–	98	~100	98
$Sc(OTf)_2$-SO_3Ph-SBA-15	NO_2–	95	~100	95
$Sc(OTf)_3$	CH_3O–	83	~100	83
$Sc(OTf)_2$-SO_3Ph-PMO	CH_3O–	86	~100	91
$Sc(OTf)_2$-SO_3Ph-SBA-15	CH_3O–	78	~100	78

[a]Reaction conditions: catalyst containing 0.025 mmol Sc, 0.50 mmol benzaldehyde or its derivatives, 1.0 mmol allyl-tri-n-butaltin, 5.0 mL H_2O, T = 80 °C, and t = 24 h. [b]100 mg $NaSO_3Ph$-PMO sample.

dx.doi.org/10.1021/sc400391r | ACS Sustainable Chem. Eng. 2014, 2, 486–492

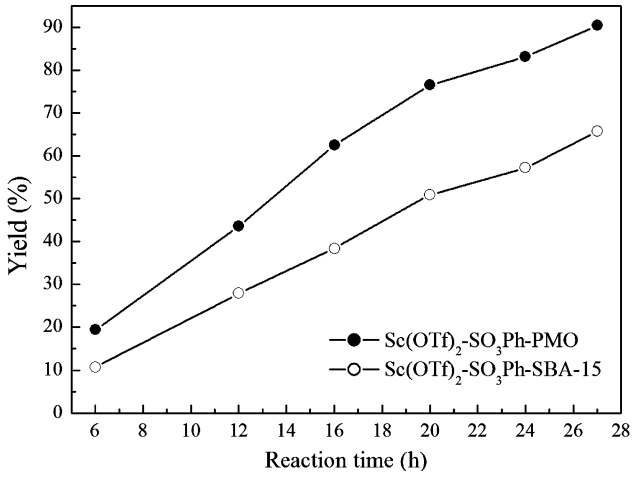

Figure 6. Reaction profile of $Sc(OTf)_2$-SO_3Ph-PMO and $Sc(OTf)_2$-SO_3Ph-SBA-15 catalysts in a water medium Mukaiyama–Aldol reaction. Reaction conditions are given in the Experimental Section.

activity of the $Sc(OTf)_2$-SO_3Ph-PMO catalyst, we first analyzed the mesoporous structure and chemical composition of the control catalyst $Sc(OTf)_2$-SO_3Ph-SBA-15. The XRD pattern and TEM image of the $Sc(OTf)_2$-SO_3Ph-SBA-15 catalyst confirmed a 2D ordered hexagonal mesostructure, which was similar to that of the $Sc(OTf)_2$-SO_3Ph-PMO catalyst (Figure S1, Supporting Information). Meanwhile, XPS spectra (Figure S2, Supporting Information) of the $Sc(OTf)_2$-SO_3Ph-SBA-15 catalyst revealed that it had almost the same Sc and S binding energy as those of the $Sc(OTf)_2$-SO_3Ph-PMO catalyst, demonstrating a similar chemical microenvironment. Therefore, the excellent catalytic efficiency of the $Sc(OTf)_2$-SO_3Ph-PMO catalyst was probably due to the existing hydrophobic microenvironment, which enriched the organic reactants and thus led to enhanced activity. In order to prove the above hypothesis, benzaldehyde substance adsorption tests in water over the $Sc(OTf)_2$-SO_3Ph-PMO and $Sc(OTf)_2$-SO_3Ph-SBA-15 catalysts were measured. The adsorption capacities of $Sc(OTf)_2$-SO_3Ph-PMO and $Sc(OTf)_2$-SO_3Ph-SBA-15 catalysts were 38% and 32%, respectively (Figure 7). Meanwhile, it could be found that the former adsorbed benzaldehyde more rapidly.

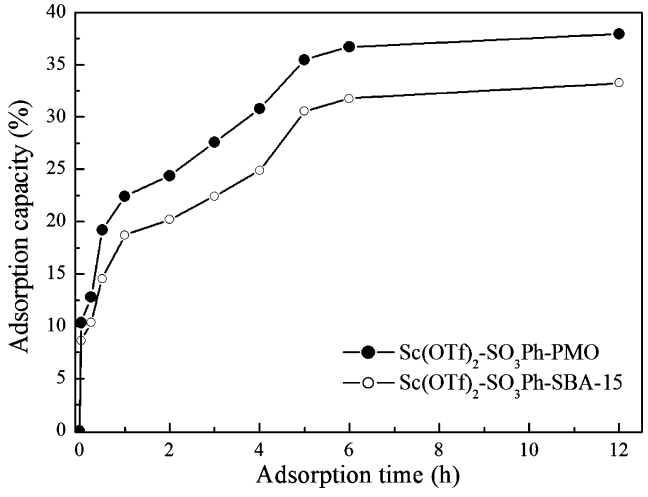

Figure 7. Benzaldehyde adsorption files of $Sc(OTf)_2$-SO_3Ph-PMO and $Sc(OTf)_2$-SO_3Ph-SBA-15 catalysts.

Therefore, the higher enrichment capacity and fast adsorption rate for the organic substances were responsible for the excellent catalytic performance of the $Sc(OTf)_2$-SO_3Ph-PMO catalyst for carbon–carbon coupling reactions in water.[47]

To determine whether the heterogeneous or the leaching scandium triflate was the real catalytic active site in $Sc(OTf)_2$-SO_3Ph-PMO catalys, we carried out the control experiment proposed by the Sheldon group.[48] After the conversion in the Barbier–Grignard reaction between benzaldehyde and allyl-tri-n-butaltin reached 50%, the mixture was centrifuged to discharge the $Sc(OTf)_2$-SO_3Ph-PMO catalyst and subsequently permitted the remaining liquor to react for another 12 h. We found that both the benzaldehyde conversion and 1-phenyl-3-buten-1-ol yield did not change with the increase in time, suggesting that the catalytic reactivity by the leaching Sc complex could be excluded in the present coupling reactions.

One of the most important issues for solid Lewis acid catalysts is their stability in water. Figure 8 shows the

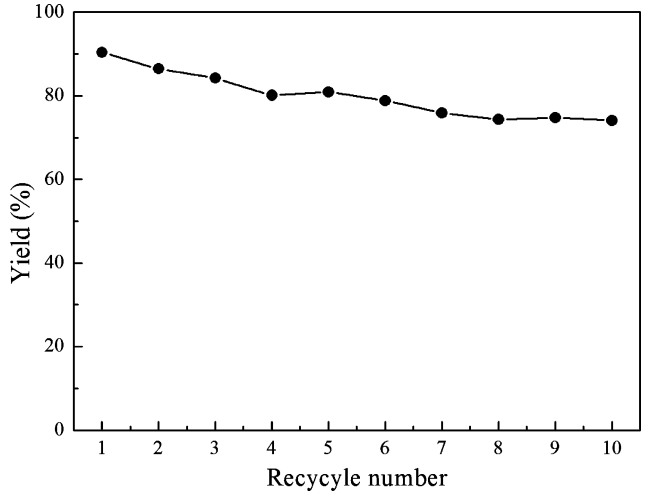

Figure 8. Recyclability of $Sc(OTf)_2$-SO_3Ph-PMO catalyst in a water medium Mukaiyama–Aldol reaction between benzaldehyde and trimethyl(1-phenylprop-1-enyloxy)silane. Reaction conditions are given in the Experimental Section.

recyclability of the $Sc(OTf)_2$-SO_3Ph-PMO catalyst during a water medium Mukaiyama–Aldol reaction between benzaldehyde and trimethyl(1-phenylprop-1-enyloxy)silane. No remarkable decrease could be found in the catalytic activity after being used repetitively 10 times, revealing its superiority over the corresponding $Sc(OTf)_3$ homogeneous catalyst for reducing cost and diminishing environmental pollution from heavy metal ions. XPS data (Figure 9a,b) of the $Sc(OTf)_2$-SO_3Ph-PMO catalyst after 10 runs displayed a similar binding energy value, suggesting an unchanged coordinated microenvironment. Moreover, the recycled $Sc(OTf)_2$-SO_3Ph-PMO catalyst displayed a slightly decreased Sc loading, S_{BET}, V_P, and D_P copared to the fresh $Sc(OTf)_2$-SO_3Ph-PMO (Table 1). The small-angle XRD pattern of the recycled $Sc(OTf)_2$-SO_3Ph-PMO catalyst (Figure S3a, Supporting Information) showed a slight decreased density of the (100) reflection. Moreover, the $Sc(OTf)_2$-SO_3Ph-PMO catalyst still exhibited type IV N_2 sorption isotherms with a H_1 hysteresis loop (Figure S3b, Supporting Information). In addition, the TEM image of the reused $Sc(OTf)_2$-SO_3Ph-PMO catalyst also exhibited a uniform mesoporous structure (Figure 9c,d) as a result of its excellent stability in water medium chemical transformations. These

dx.doi.org/10.1021/sc400391r | ACS Sustainable Chem. Eng. 2014, 2, 486–492

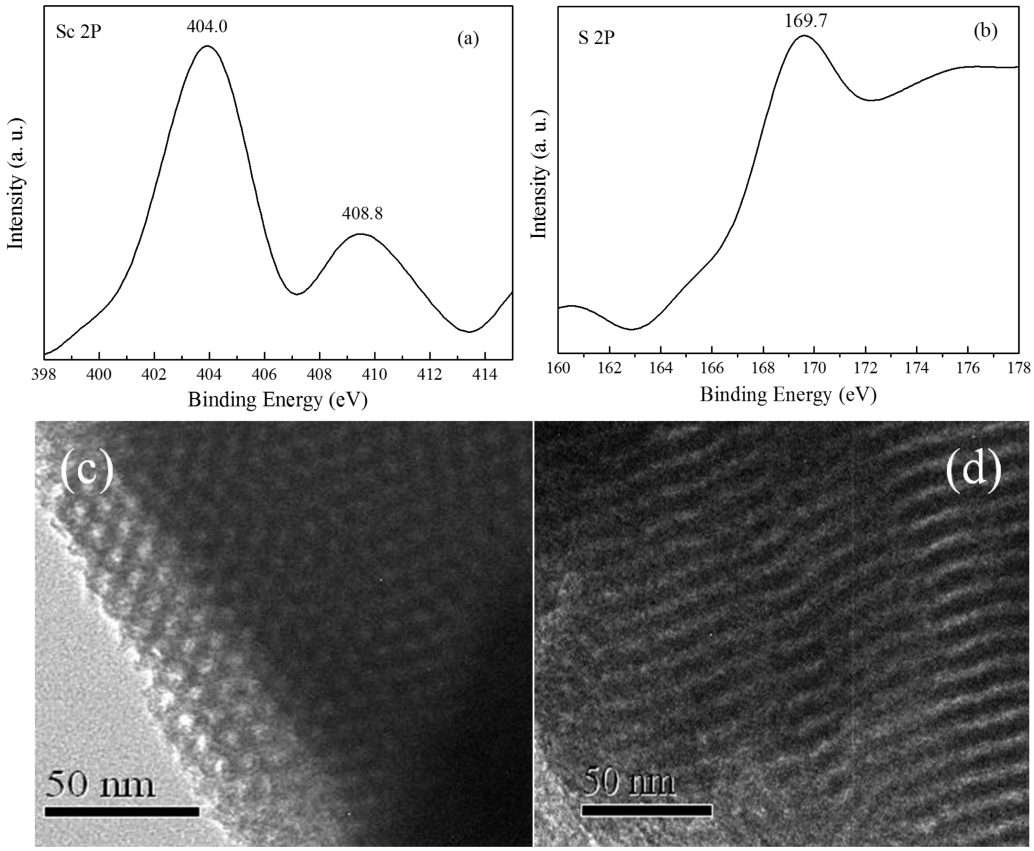

Figure 9. XPS spectra (a,b) and TEM images (c,d) of the recycled $Sc(OTf)_2$-SO_3Ph-PMO catalyst.

results confirmed that the ordered degree of the mesoporous structure for the recycled $Sc(OTf)_2$-SO_3Ph-PMO catalyst had only a slight decrease after 10 reuses.

CONCLUSION

In conclusion, a new periodic mesoporous Sc Lewis acid catalyst was successfully synthesized by immobilizing scandium triflate into sodium benzenesulfonate-functionalized periodic mesoporous silica. It showed much higher reactivity in the water medium Barbier–Grignard and Mukaiyama–Aldol reactions compared to those of the homogeneous catalyst $Sc(OTf)_3$ and control catalyst $Sc(OTf)_2$-SO_3Ph-SBA-15. This excellent catalytic reactivity could be attributed to its intrinsic properties resulting from mesoporosity and the hydrophobic microenvironment. Meanwhile, it also displayed excellent stability in water and could be reused 10 times with a slight loss of catalytic efficiency. This novel approach could be used for the synthesis of highly active solid Lewis acid catalysts for various aqueous organic transformations.

ASSOCIATED CONTENT

Supporting Information

XRD pattern, N_2 sorption isotherm, XPS spectrum, and TEM image of the $Sc(OTf)_2$-SO_3Ph-SBA-15 catalyst. This material is available free of charge via the Internet at http://pubs.acs.org.

AUTHOR INFORMATION

Corresponding Authors

*E-mail: zhangfang@shnu.edu.cn (F.Z.).
*E-mail: HeXing-Li@shnu.edu.cn (H.L.).

Notes

The authors declare no competing financial interest.

ACKNOWLEDGMENTS

This work is supported by the Natural Science Foundation of China (21107071 and 51273112), PCSIRT (IRT1269), and Shanghai Government (10dj1400100 and 13QA1402800).

REFERENCES

(1) Song, C. S. Global challenges and strategies for control, conversion and utilization of CO_2 for sustainable development involving energy, catalysis, adsorption and chemical processing. *Catal. Today* **2006**, *115*, 2–32.
(2) Sheldon, R. A.; Arends, I.; Hanefeld, U. *Green Chemistry and Catalysis*; Wiley: Weinheim, 2007.
(3) Sheldon, R. A.; Downing, R. S. Heterogeneous catalytic transformations for environmentally friendly production. *Applied Catal., A* **1999**, *189*, 163–183.
(4) Corma, A.; García, H. Lewis acids: From conventional homogeneous to green homogeneous and heterogeneous catalysis. *Chem. Rev.* **2003**, *103*, 4307–4365.
(5) Minakata, S.; Komatsu, M. Organic reactions on silica in water. *Chem. Rev.* **2009**, *109*, 711–724.
(6) Lamblin, M.; Nassar-Hardy, L.; Hierso, J.; Fouquet, E.; Felpin, F. Recyclable heterogeneous palladium catalysts in pure water: Sustainable developments in Suzuki, Heck, Sonogashira and Tsuji–Trost reactions. *Adv. Syn. Catal.* **2010**, *352*, 33–79.
(7) Uozumi, Y.; Matsuura, Y.; Arakawa, T.; Yamada, Y. M. A. Asymmetric Suzuki–Miyaura coupling in water with a chiral palladium catalyst supported on an amphiphilic resin. *Angew. Chem., Int. Ed.* **2009**, *48*, 2708–2710.
(8) Li, C. J. Organic reactions in aqueous media with a focus on C–C bond formations: A decade update. *Chem. Rev.* **2005**, *105*, 3095–3165.

(9) Lindström, U. M. Stereoselective organic reactions in water. *Chem. Rev.* **2002**, *102*, 2751−2772.
(10) Chanda, A.; Fokin, V. V. Organic synthesis "on water". *Chem. Rev.* **2009**, *109*, 725−748.
(11) Butler, R. N.; Coyne, A. G. Water: Nature's reaction enforcer—Comparative effects for organic synthesis "in-water" and "on-water. *Chem. Rev.* **2010**, *110*, 6302−6337.
(12) Inumaru, K.; Ishiharam, T.; Kamiya, Y.; Okuhara, T.; Yamanaka, S. Water-tolerant, highly active solid acid catalysts composed of the Keggin-type polyoxometalate $H_3PW_{12}O_{40}$ immobilized in hydrophobic nanospaces of organomodified mesoporous silica. *Angew. Chem., Int. Ed.* **2007**, *46*, 7625−7628.
(13) Kobayashi, S.; Manabe, K. Development of novel Lewis acid catalysts for selective organic reactions in aqueous media. *Acc. Chem. Res.* **2002**, *35*, 209−217.
(14) Kobayashi, S.; Sugiura, M.; Kitagawa, H.; Lam, W. W.-L. Rare-earth metal triflates in organic synthesis. *Chem. Rev.* **2002**, *102*, 2227−2302.
(15) Liu, Y.; Mo, K.; Cui, Y. Porous and robust lanthanide metal-organoboron frameworks as water tolerant Lewis acid catalysts. *Inorg. Chem.* **2013**, *52*, 10286−10291.
(16) Kobayashi, S.; Nagayama, S. A microencapsulated Lewis acid. A new type of polymer-supported Lewis acid catalyst of wide utility in organic synthesis. *J. Am. Chem. Soc.* **1998**, *120*, 2985−2986.
(17) Gu, W. Q.; Zhou, W. J.; Gin, D. L. A nanostructured, scandium-containing polymer for heterogeneous Lewis acid catalysis in water. *Chem. Mater.* **2001**, *13*, 1949−1951.
(18) Nagayama, S.; Kobayashi, S. A novel polymer-supported scandium catalyst which shows high activity in water. *Angew. Chem., Int. Ed.* **2000**, *39*, 567−569.
(19) Reetz, M. T.; Giebel, D. Cross-linked scandium-containing dendrimers: A new class of heterogeneous catalysts. *Angew. Chem., Int. Ed.* **2000**, *39*, 2498−2501.
(20) Karimi, B.; Ma'Mani, L. A highly efficient and recyclable silica-based scandium(III) interphase catalyst for cyanosilylation of carbonyl compounds. *Org. Lett.* **2004**, *6*, 4813.
(21) Takeuchi, M.; Akiyama, R.; Kobayashi, S. Polymer-micelle incarcerated scandium as a polymer-supported catalyst for high-throughput organic synthesis. *J. Am. Chem. Soc.* **2005**, *127*, 13096−13097.
(22) Xu, Y. J.; Gu, W. Q.; Gin, D. L. Heterogeneous catalysis using a nanostructured solid acid resin based on lyotropic liquid crystals. *J. Am. Chem. Soc.* **2004**, *126*, 1616−1617.
(23) Gu, Y. L.; Ogawa, C.; Kobayashi, S. Silica-supported sodium sulfonate with ionic liquid:□ A neutral catalyst system for Michael reactions of indoles in water. *Org. Lett.* **2007**, *9*, 175−178.
(24) Olmos, A.; Alix, A.; Sommer, J.; Pale, P. Sc(III)-doped zeolites as new heterogeneous catalysts: Mukaiyama Aldol reaction. *Chem.—Eur. J.* **2009**, *15*, 11229−11234.
(25) Gu, Y. L.; Ogawa, C.; Kobayashi, J.; Mori, Y.; Kobayashi, S. A heterogeneous silica-supported scandium/ionic liquid catalyst system for organic reactions in water. *Angew. Chem., Int. Ed.* **2006**, *45*, 7217−7220.
(26) Román-Leshkov, Y.; Davis, M. E. Activation of carbonyl-containing molecules with solid Lewis acids in aqueous media. *ACS Catal.* **2011**, *1*, 1566−1580.
(27) Surya Prakash, G. K.; Mathew, T.; Olah, G. A. Gallium(III) triflate: An efficient and a sustainable Lewis acid catalyst for organic synthetic transformations. *Acc. Chem. Res.* **2012**, *45*, 565−577.
(28) Wang, Y.; Wang, F.; Song, Q.; Xin, Q.; Xu, S.; Xu, J. Heterogeneous ceria catalyst with water-tolerant Lewis acidic sites for one-pot synthesis of 1,3-diols via Prins condensation and hydrolysis reactions. *J. Am. Chem. Soc.* **2013**, *135*, 1506−1515.
(29) Khalafi-Nezhad, A.; Haghighi, S.; Panahi, F. Nano-TiO_2 on dodecyl-sulfated silica: As an efficient heterogeneous Lewis acid-surfactant-combined catalyst (HLASC) for reaction in aqueous media. *ACS Sustainable Chem. Eng.* **2013**, *1*, 1015−1023.
(30) Van Der Voort, P.; Esquivel, D.; De Canck, E.; Goethals, F.; Van Driessche, I.; J. Romero-Salguero, F. Periodic mesoporous organosilicas: From simple to complex bridges; a comprehensive overview of functions, morphologies and applications. *Chem. Soc. Rev.* **2013**, *42*, 3913−3955.
(31) Wang, W. D.; Lofgreen, J. E.; Ozin, G. A. Why PMO? Towards functionality and utility of periodic mesoporous organosilicas. *Small* **2010**, *6*, 2634−2642.
(32) Yang, Q. H.; Liu, J.; Zhang, L.; Li, C. Functionalized periodic mesoporous organosilicas for catalysis. *J. Mater. Chem.* **2009**, *19*, 1945−1955.
(33) Inagaki, S.; Guan, S.; Ohsuna, T.; Terasaki, O. An ordered mesoporous organosilica hybrid material with a crystal-like wall structure. *Nature* **2002**, *416*, 304−307.
(34) A. Melero, J.; van Grieken, R.; Morales, G. Advances in the synthesis and catalytic applications of organosulfonic-functionalized mesostructured materials. *Chem. Rev.* **2006**, *106*, 3790−3812.
(35) Karimi, B.; Mirzaei, H.; Mobaraki, A. Periodic mesoporous organosilica functionalized sulfonic acids as highly efficient and recyclable catalysts in biodiesel production. *Catal. Sci. Technol.* **2012**, *2*, 828−834.
(36) Siegel, R.; Domingues, E.; De Sousa, R.; Jérôme, F.; Morais, C. M.; Bion, N.; Ferreira, P.; Mafra, L. Understanding the high catalytic activity of propylsulfonic acid-functionalized periodic mesoporous benzenesilicas by high-resolution ^{1}H solid-state NMR spectroscopy. *J. Mater. Chem.* **2012**, *22*, 7412−7419.
(37) Sreekanth, P.; Kim, S.; Hyeon, T.; Kim, B. A novel mesoporous silica-supported Lewis acid catalyst for C−C bond formation reactions in water. *Adv. Synth. Catal.* **2003**, *345*, 936−938.
(38) Mantri, K.; Komura, K.; Kubota, Y.; Sugi, Y. Friedel−Crafts alkylation of aromatics with benzyl alcohols catalyzed by rare earth metal triflates supported on MCM-41 mesoporous silica. *J. Mol. Catal. A: Chem.* **2005**, *236*, 168−175.
(39) Candu, N.; Ciobanu, M.; Filip, P.; EI Haskouri, J.; Guillem, C.; Amoros, P.; Beltran, D.; Coman, S.; Parvulescu, V. Efficient Sc triflate mesoporous-based catalysts for the synthesis of 4,4′-methylenedianiline from aniline and 4-aminobenzylalcohol. *J. Catal.* **2012**, *287*, 76−85.
(40) Kumar, R.; Sharma, J. P.; Sekhon, S. S. FTIR study of ion dissociation in PMMA based gel electrolytes containing ammonium triflate: Role of dielectric constant of solvent. *Eur. Polym. J.* **2005**, *41*, 2718−2725.
(41) Kawabata, T.; Mizugaki, T.; Ebitani, K.; Kaneda, K. A novel montmorillonite-enwrapped scandium as a heterogeneous catalyst for Michael reaction. *J. Am. Chem. Soc.* **2003**, *125*, 10486−10487.
(42) Zhang, F.; Liang, C.; Chen, M. Z.; Guo, H. B.; Jiang, H. Y.; Li, H. X. An extremely stable and highly active periodic mesoporous Lewis acid catalyst in water-medium Mukaiyama-aldol reaction. *Green Chem.* **2013**, *15*, 2865−2871.
(43) Yang, Q. H.; Kapoor, M. P.; Inagaki, S. Sulfuric acid-functionalized mesoporous benzene-silica with a molecular-scale periodicity in the walls. *J. Am. Chem. Soc.* **2002**, *124*, 9694−9695.
(44) Zhao, D. Y.; Feng, J. L.; Huo, Q. S.; Melosh, N.; Fredrickson, G. H.; Chmelka, B. F.; Stucky, G. D. Triblock copolymer syntheses of mesoporous silica with periodic 50 to 300 angstrom pores. *Science* **1998**, *279*, 548−552.
(45) Margolese, A.; Melero, S. C.; Christiansen, B. F.; Stucky, G. D. Direct syntheses of ordered SBA-15 mesoporous silica containing sulfonic acid groups. *Chem. Mater.* **2000**, *12*, 2448−2459.
(46) Nakajima, K.; Tomita, I.; Hara, M.; Hayashi, S.; Domen, K.; Kondo, J. N. A stable and highly active hybrid mesoporous solid acid catalyst. *Adv. Mater.* **2005**, *17*, 1839−1842.
(47) Fu, W. Q.; Zhang, L.; Tang, T. D.; Ke, Q. P.; Wang, S.; Hu, J. B.; Fang, G. Y.; Li, J. X.; Xiao, F. S. Extraordinarily high activity in the hydrodesulfurization of 4,6-dimethyldibenzothiophene over Pd supported on mesoporous zeolite Y. *J. Am. Chem. Soc.* **2011**, *133*, 15346−15349.
(48) Sheldon, R. A.; Wallau, M. I.; Arends, W. C. E.; Schuchardt, U. Heterogeneous catalysts for liquid-phase oxidations: Philosophers'-stones or trojan horses? *Acc. Chem. Res.* **1998**, *31*, 485−493.